Naval Research Laboratory

Washington, DC 20375-5320

NRL/MR/5708--20-10,099

Models for Transient Heat-Sink Controlled Temperature Fields within Layered Materials

Edward PA Michaelchuck, Jr.

Scott A. Ramsey

Troy Mayo

Signature Technology Office
Tactical Electronic Warfare Division

Samuel G. Lambrakos

Center for Materials Physics & Technology Branch
Materials Science & Technology Division

October 11, 2020

REPORT DOCUMENTATION PAGE

Form Approved
OMB No. 0704-0188

1. REPORT DATE *(DD-MM-YYYY)*	**2. REPORT TYPE**	**3. DATES COVERED** *(From - To)*
11-10-2020	NRL Memorandum Report	

4. TITLE AND SUBTITLE

Models for Transient Heat-Sink Controlled Temperature Fields within Layered Materials

5a. CONTRACT NUMBER

5b. GRANT NUMBER

5c. PROGRAM ELEMENT NUMBER

6. AUTHOR(S)

Edward PA Michaelchuck, Jr., Scott A. Ramsey, Troy Mayo, and Samuel G. Lambrakos

5d. PROJECT NUMBER

5e. TASK NUMBER
0010

5f. WORK UNIT NUMBER
100001558391

7. PERFORMING ORGANIZATION NAME(S) AND ADDRESS(ES)

Naval Research Laboratory
4555 Overlook Avenue, SW
Washington, DC 20375-5320

8. PERFORMING ORGANIZATION REPORT NUMBER

NRL/MR/5708--20-10,099

9. SPONSORING / MONITORING AGENCY NAME(S) AND ADDRESS(ES)

US Special Operations Command, Special Operations Forces Acquisition, Technology, and Logistics
7701 Tampa Point Blvd
MacDill Air Force Base, Florida 33621

10. SPONSOR / MONITOR'S ACRONYM(S)

USSOCOM SOF AT&L

11. SPONSOR / MONITOR'S REPORT NUMBER(S)

12. DISTRIBUTION / AVAILABILITY STATEMENT

DISTRIBUTION STATEMENT A: Approved for public release; distribution is unlimited.

13. SUPPLEMENTARY NOTES

14. ABSTRACT

Parametric modeling of layer-configuration and heat-sink controlled temperature fields within layered materials is examined. This modeling is in terms of the heat-kernel solution to the heat conduction equation with the introduction of finite layers of varying thermal diffusivities and a negative thermal impulse, of the heat kernel form, for the introduction of singular heat-sink layers. This provides phenomenological parametric representations of temperature distributions within layered-material systems and can be utilized for their design and optimization for layer-configuration and heat-sink control of thermal transport. Results of prototype modeling of controlled heat transfer in layered-material systems are presented, demonstrating general aspects of parametric models for thermal analysis and simulation of heat-transfer control using layer configurations and embedded heat sinks.

15. SUBJECT TERMS

Parametric model
Layered materials
Heat sink
Heat transfer

16. SECURITY CLASSIFICATION OF:			**17. LIMITATION OF ABSTRACT**	**18. NUMBER OF PAGES**	**19a. NAME OF RESPONSIBLE PERSON**
					Edward Michaelchuck
a. REPORT	**b. ABSTRACT**	**c. THIS PAGE**	Unclassified Unlimited	22	**19b. TELEPHONE NUMBER** *(include area code)*
Unclassified Unlimited	Unclassified Unlimited	Unclassified Unlimited			(202) 279-5233

This page intentionally left blank.

Introduction

The need to control heat transfer through multilayer materials is ubiquitous and *multidisciplinary* with respect to applications. These applications range from control of volumetric heat deposition for surface treatment of materials to thermal management of systems, where there can be localized high-temperature regions resulting in system degradation. Optimizing heat transfer through multilayer materials requires estimating the thermal response of layered composite materials whose fabrication is both feasible and operationally practical. Accordingly, parametric models that combine heat-transfer characteristics and thermal material properties, enabling prediction of temperature fields within multilayer materials, should be well posed. These models should be conveniently adaptable for estimating the thermal response of different types of layered materials.

A general approach for control of heat transfer through multilayer materials is that of system design that includes heat sinks as embedded layers. This approach is motivated by welding processes, where work piece temperatures are controlled by thermal contact to base plates, and by electronic system designs requiring thermal management. [1] Parametric modeling of heat-sink controlled heat transfer can be based on modeling energy flow through a system via a thermal impulse and removing a specified amount of energy from the system via a negative thermal impulse at a specified location. The mathematical foundation is that of Green's functions and the inverse thermal-analysis approach, where parametric models provide for inclusion of information concerning the physical characteristics of heat-transfer processes. The present study concerns parametric modeling of a layered material system including heat-sink controlled heat transfer. This system is inherently *multiscale* in nature, and therefore, poses a specific problem with respect to parametric modeling. A schematic representation of the multiscale characteristics of layer-configuration and heat-sink controlled heat transfer in layered-material systems is given in Figure 1, where the heat-sink layer is assumed to have a thermal diffusivity that is significantly larger than those other layers comprising the system. Referring to Figure 1, for the purpose of parametric modeling, layer-configuration and heat-sink controlled heat transfer in layered-materials can be represented as occurring on three different length scales.

Manuscript approved Month 00, 2020.

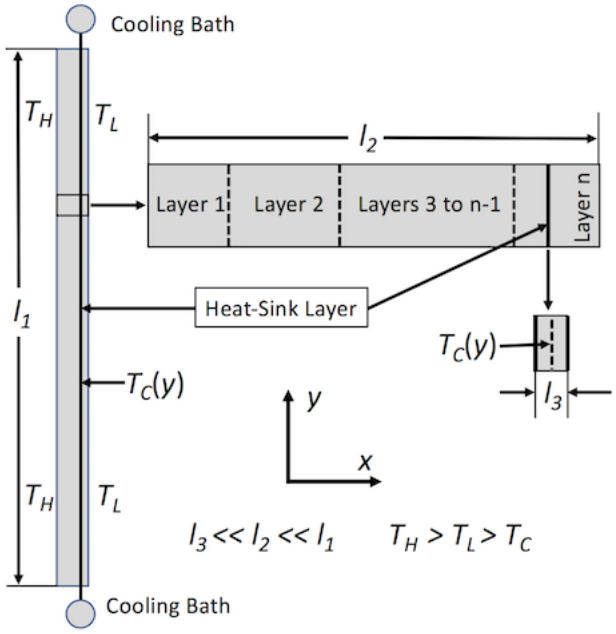

Figure 1. Schematic representation of multiscale characteristics of layer and heat-sink controlled heat transfer in layered materials, where T_H and T_L are temperatures of hot body and ambient atmosphere, respectively, and $T_C(y)$ is temperature of heat sink at location y, along the heat-sink layer relative to the cooling bath.

The general physical character of heat sinks is that their thermal diffusivities are substantially greater than those of the workpieces whose temperature fields are to be controlled. Accordingly, thermal coupling of heat sinks to adjacent layers is such that regions of temperature fields close to and within heat sinks can be represented by a negative thermal impulse. [1]

The goal of parametric modeling is the generation of a parameter space for estimating optimal parameter values for a given system specification. The parameter space should be an encoding of material response functions (e.g., effective thermal diffusivities) that are achievable for realistic system design. For complex material systems, the determination of material response functions is well posed in terms of inverse analysis. The multiscale character of layer and heat-sink control represented by Figure 1 defines three inverse problems, with respect to which the parametric models can be applied for inverse analysis. These inverse problems follow from the realization that layered-material thermal properties are not the same as those of bulk materials. First, referring to Figure 1, it should be noted that heat transfer within the heat-sink layer, which is along scale l_1, is that of a thin-layer material, coupled to adjacent material surfaces. The thermal diffusivity for heat transfer with respect to scale l_1 should be a complex function of different physical variables, and in general better determined by inverse analysis, rather than approximated using bulk properties. Next, referring to Figure 1, heat transfer along scale l_2, within a complex multilayer material, is characterized by multiple material interfaces. Again, thermal diffusivity for heat transfer with respect to scale l_2 is not that characteristic of a uniform bulk material having known thermal properties, and thus should be determined by inverse analysis. In particular, for layer and heat-sink control of temperature fields within layered materials, there is typically thermal transport due to advection at bounding surfaces of the layered system. Accordingly, parametrization should

be extended to include effective diffusivities, which are based formally on replacing the advection-diffusion operator with an effective-diffusion operator, i.e.,

$$\kappa \frac{d^2T}{dx^2} - V \frac{dT}{dx} = \kappa_{eff} \frac{d^2T}{dx^2} \quad \text{Eq. 1}$$

Where V specifies the material flow field and κ_{eff} is the effective diffusivity, which represents the combined influence of both thermal diffusion and advection. Physically, advection is not expected to manifest as influencing thermal transport locally within a layered-material system but rather as influencing thermal transport over the its entire length l_2. Accordingly, the phenomenological influence of advection, which is associated with ambient environments at surface boundaries of a layered-material system, again poses a problem of inverse thermal analysis for determination of effective diffussivities. Finally, referring to Figure 1, heat transfer along scale l_3, the heat-sink layer, is effectively singular with respect to scales l_1 and l_2 because of the relatively large thermal diffusivity of this layer. Accordingly, with respect to parametric modeling, this layer can be represented by an effective heat-sink source having singular characteristics with respect to heat transfer. Heat transfer to the localized heat-sink layer from adjacent layers of material will depend on the characteristic thermal coupling of layer interfaces, which again is a complex material property, not known *a priori*, and thus appropriately posed for inverse thermal analysis. The singular nature of heat-sink coupling was demonstrated in Reference 2. [2] In addition to providing quantitative estimation by means of inverse thermal analysis, parametric modeling can provide qualitative estimation of system response. For example, in the case of layer-configuration and heat-sink controlled heat transfer in layered-materials, what general design goals can be achieved by adjusting qualitatively relative locations and diffusivities of layers.

The purpose of this analysis is to present a modification to the heat-kernel solution which includes the effects of multiple layers with varying thermal diffusivities, interface effects (e.g., large changes in thermal properties), contact resistance, and the effects of singular heat-sinks that are represented by a negative thermal impulse. Organization of subject areas presented are as follows. First, parametric models of temperature fields for layer and heat-sink controlled heat transfer in layered materials are presented. Second, prototype analyses using parametric models are described. Finally, a discussion and conclusion are given.

Parametric Models

The parametric models presented in this section are phenomenological generalizations of the analytical solution to the heat conduction equation for heat transfer through a boundary between regions having different thermal properties [3]. The solutions presented here are not bounded; therefore, the region extends from negative infinity to positive infinity. The heat sink models parametrically represent a 2-D system in 1-D due to the convenience of parameter optimization in 1-D. The 2-D heat transfer along the heat sink layer is represented by an effective heat-sink source having singular characteristics with respect to heat transfer. Note that although this representation of the heat sink is that of a negative thermal impulse, it is possible to represent the heat sink by an effective diffusivity over a thin, finite layer. The heat sink's effective diffusivity must be independently determined for use in the following parametric models as an input parameter. The parametric models are formulated for simulating unsteady evolution of the temperature field via

modifications to the heat-kernel solution to the heat conduction equation. The analysis in this study considers evolution of a delta function impulse at time zero (i.e., heat kernel solution) propagating through a layered system with an initial ambient temperature profile, T_A. The heat-kernel solution presented here propagates from position zero to infinity. Note that the multi-layer material slabs presented below are considered to be a finite when $N_0<N<N_k$. The first layer and last layer of the material is considered to be an infinite medium in the half-space.

Model 1. Shown in Figure 2 is a schematic representation of Model 1.

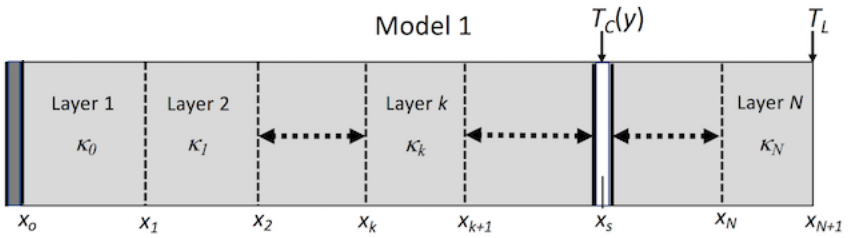

Figure 2. Schematic representation of Model 1.

For layer and heat-sink control of unsteady temperature fields within layered materials for a delta impulse of energy, where effects due to changes in diffusivity at layer interfaces are assumed small, parametric representation in terms the heat-kernel solution is of the form

$$T(\hat{x},t) = G_1(x,x_0,\beta,t,t_0) - G_s(x,x_s,\kappa_s,t,t_s) + T_A \qquad \text{Eq. 2}$$

Where

$$G_1(x,x_0,\beta,t,t_0) = \frac{u(t-t_0)\cdot C(x_0)}{\sqrt{4\pi\cdot\kappa_0\cdot(t-t_0)}} e^{-\frac{\beta^2}{4\cdot(t-t_0)}} \qquad \text{Eq. 3}$$

$$G_s(x,x_s,\kappa_s,t,t_s) = \frac{u(t-t_s)\cdot C_s(x_s)}{\sqrt{4\pi\cdot\kappa_s\cdot(t-t_s)}} e^{-\frac{(x-x_s)^2}{4\cdot\kappa_s\cdot(t-t_s)}} \qquad \text{Eq. 4}$$

$$\beta = \frac{x-x_n}{\sqrt{\kappa_k}} + \sum_{i=0}^{N_k-1} \frac{x_{i+1}-x_i}{\sqrt{\kappa_i}} \qquad \text{Eq. 5}$$

for $x_{n+1} \geq x \geq x_n$, and

$$T(\hat{x}_n^c, t_n^c) = T_n^c \qquad \text{Eq. 6}$$

$$Z_T = \sum_{n=1}^{N} w_n \left(T(\hat{x}_n^c, t_n^c) - T_n^c \right)^2 \qquad \text{Eq. 7}$$

The quantities T_A, $C(x_0)$, $C_s(x_s)$, κ_s, κ_k (k = 1,..., N_k), t, and $u(t)$ are the ambient temperature, arbitrary scaling parameter, effective diffusivities of the layered system, effective diffusivity of the heat-sink, time, and unit step function, respectively [1]. Note that β, x_n, and N_k are path weighted thermal diffusivity, the layer interface behind of the current spatial position, and the number of layers up to the current spatial position. The parametric model Eqs. 2-4 (Model 1) adopts $C(x_0)$, $C_s(x_s)$, κ_s, and κ_k (k = 1,..., N_L) as adjustable parameters for inverse thermal analysis and

simulation of layer-configuration and heat-sink controlled heat transfer in layered materials. Equation 3 represents the classic heat-kernel solution to the heat conduction equation where the delta impulse begins propagating at time t_0. The heat sink term is represented by Equation 2 and 4 where the heat sink effectively removes energy from the system at a specified location beigning at time t_s. Equation 5 represents the addition of multiple layers where the thermal diffusivity at any location in space, x, is a function of the diffusivities of the entire system. For the purpose of this model, the y dependence of temperature, which is with respect to the heat-sink temperature $T_c(y)$ along the coordinate axis perpendicular to heat transfer through the layer system described by Figure 1, 2, and 3, is effectively disregarded in this 1-D model space. The dependence on the y-axis location of a heat sink would effectively be captured by the equivalent source term $C(x_s)$ where the scaling parameter has been evalauted for a system at a specified y-location using inverse analysis. Note that the effects of contact resistance between layers are not explicitly shown in Model 1 because contact resistance can be expressed as an effective diffusivity determined through inverse analysis.

The locations $\hat{x}_n^c$ and temperature values T_n^c specify constraint conditions on the temperature field. Constraint conditions are imposed on the temperature field spanning the spatial domain of the layered material by minimization of the objective function defined by Eq. 7, where T_n^c is the target temperature for position $\hat{x}_n^c = (x_n^c, y_n^c, z_n^c)$. The input of information into the parametric model, defined by Eqs. 2-5 (Model 1) and Eqs. 8-15 (Model 2) presented below, is effected by the assignment of individual constraint values to the quantities T_n^c and the form of the basis functions adopted for parametric representation, which include the influence of boundary and constraint conditions (i.e., T_H, T_L, and T_C in Figure 1) and charateristic changes of thermal properties from one layer to another. The constraint conditions and parameterized basis functions provide for the inclusion of information from both laboratory and numerical experiments.

Model 2. Shown in Figure 3 is a schematic representation of Model 2.

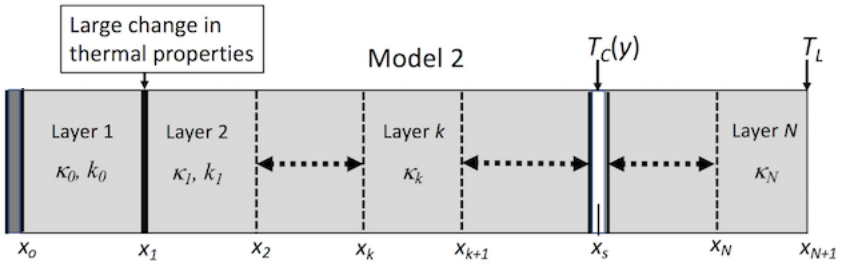

Figure 3. Schematic representation of Model 2.

For layer-configuration and heat-sink control of unsteady temperature fields within layered materials for a delta impulse of energy, where effects due to changes in diffusivity at layer interfaces are significant, parametric representation in terms of the heat-kernel solution is of the form

$$T(\hat{x}, t) = G_2(x, x_0, t, t_o) - G_s(x, x_s, \kappa_s, t, t_s) + T_A \qquad \text{Eq. 8}$$

$$G_s(x, x_s, \kappa_s, t, t_s) = \frac{u(t-t_s)\cdot C_s(x_s)}{\sqrt{4\pi\cdot\kappa_s\cdot(t-t_s)}} e^{-\frac{(x-x_s)^2}{4\cdot\kappa_s\cdot(t-t_s)}} \quad \text{Eq. 9}$$

Where, for $x < x_1$ and $x_{imag} = x + x_0 - 2x_1$,

$$G_2(x, x_0, t, t_o) = \frac{u(t-t_0)\cdot C(x_0)}{\sqrt{4\pi\cdot\kappa_0\cdot(t-t_o)}} \cdot \left[e^{-\frac{(x-x_0)^2}{4\cdot\kappa_0\cdot(t-t_o)}} + W_0 \cdot e^{-\frac{(x_{imag})^2}{4\cdot\kappa_0\cdot(t-t_0)}} \right] \quad \text{Eq. 10}$$

And for $x \geq x_1$,

$$G_2(x, x_0, t, t_o) = \frac{u(t-t_0)\cdot C(x_0)\cdot W_1}{\sqrt{\pi\cdot\kappa_1\cdot(t-t_o)}} e^{-\frac{\beta^2}{4\cdot(t-t_o)}} \quad \text{Eq. 11}$$

$$\beta = \frac{x-x_n}{\sqrt{\kappa_k}} + \sum_{i=0}^{N_k-1} \frac{x_{i+1}-x_i}{\sqrt{\kappa_i}} \quad \text{Eq. 12}$$

The layer weight coefficients W_0 and W_1 are given by

$$W_0 = \frac{k_0\sqrt{\kappa_1}-k_1\sqrt{\kappa_0}}{k_0\sqrt{\kappa_1}+k_1\sqrt{\kappa_0}} \quad \text{Eq. 13}$$

And

$$W_1 = \frac{k_0\kappa_1}{\sqrt{\kappa_0}(k_0\sqrt{\kappa_1}+k_1\sqrt{\kappa_0})} \quad \text{Eq. 14}$$

The quantities T_A, $C(x_0)$, $C_s(x_s)$, κ_s, κ_k ($k = 1,...,N_L$), t, and $u(t)$ are are defined as for Model 1. The quantities k_0 and k_1 are the effective conductivities of layers 1 and 2, respectively It should be noted that the weight coefficients W_0 and W_1 represent the reflected and transmitted heat wave due to a large change in thermal properties. Also, the coefficients defined by Eqs. 13 and 14 provide a metric for estimating the influence on thermal transport due to changes of thermal properties at interfaces between layers. Resonably small values of W_0 imply that Model 1 is applicable for analysis or simulation of layered-material heat transfer. In particular, Eq. 5 provides reasonably accurate representation of changes in effective diffusivity as a function of layer.

Referring to Figure 3, the interface between layers, having large differences in effective diffusivities, can be placed at any position within the layered system. In which case, the effective diffusivity κ_0 would be replaced by that determined using Eq. 15 and the k_0 would be replaced by an effective conductivity given by Eqs. 16 and 17.

$$\kappa_k = \frac{(x-x_0)^2}{\beta^2} \quad \text{Eq. 15}$$

$$\gamma = \frac{x-x_n}{\sqrt{k_k}} + \sum_{i=1}^{n-1} \frac{x_{i+1}-x_i}{\sqrt{k_i}} \quad \text{Eq. 16}$$

$$k_k = \frac{(x-x_0)^2}{\gamma^2} \quad \text{Eq. 17}$$

Note that the effects of contact resistance between layers are not explicitly shown in Model 2 because contact resistance can be expressed as an effective diffusivity determined through inverse analysis. Additionally, contact resistance can be explicitly represented by Eq. 10 where the weighting functions, W_0 and W_1, account for the contact resistance between layers.

The parametric models presented here, Models 1 and 2, specify a general procedure for parametric modeling of unsteady temperature fields in layered-material systems. These parametric models are characterized by the classic heat-kernal solution coupled with a layered material system and negative heat-sink source. The mathematical foundation of Models 1 and 2 is a discrete representation of a parabolic partial differential equation which is consistent with the physical characteristics of unsteady heat conduction that is unconditionally stable [11].

Heat-Sink Controlled Temperature Fields

This section describes a series of computational experiments describing parametric modeling of layer-configuration and heatsink-controlled thermal transport within layered material systems. The design of these experiments, which uses physically realistic thermal properties, was not for demonstrating optimal materials for layer-configuration and heat-sink thermal control, which is certainly beyond the scope of this study, but rather general characteristics of the parametric models for modeling and simulation of such control, as well as demonstrating feasibily of such control using multilayer and heat-sink materials. The computational experiments described in this section represent thermal analysis/simulations; however, inverse thermal anaylsis would be required for real world application, the goal of parametric modeling.

The thermal simulations as posed here assume a complex interaction between a heating surface in the form of a delta impulse of energy and a multilayer material where all of the complex interactions are treated as effective thermal diffusivities, e.g. convective and radiative heat transfer are treated as an effective thermal diffusivity. For example, the interaction of a heating body and multilayer material can involve flow of material through porous microstructure within layers and subsequent evaporation at the outer surface. A first estimate of the thermal response of a layered system using inverse analysis, without consideration of details concerning multilayer characteristics and heat-sink-layer coupling, is determination of an effective diffusivity averaged over a single layer.

For the prototype thermal analyses presented below, it was assumed that determination of effective diffusivities was according to an experimentally measured boundary value T_H and an experimentally measured heat sink temperature reduction, T_S, as well as other assumed system characteristics.

Model 1. A first estimate of the thermal response of a layered system using Model 1, without consideration of details concerning multilayer characteristics and heat-sink-layer coupling, is evaluating the effects of thermal diffusivities on temperature distribution over time. Here the effective diffusivities (e.g., κ_0 (polypropylene, $9.6 \cdot 10^{-8}$ $m^2 s^{-1}$)) are assumed to be determined according to experimentally measured boundary values T_H and T_L of the layer-material diffusivity without boundary and microstructural influences. Note that in the following simulations, Figures

4-12, that the first layer extends to negative infinity, and the last layer extends to positive infinity. The graphs have been clipped at a specified distance for graphical presentation purposes. The thermal pulse has been scaled, via the arbitrary scaling parameter $C(x_0)$, to a magnitude of $100^{O}C$ at $T(0, t_0)$, but the pulse at t_0 will only be shown in Figure 4 for graphical presentation purposes.

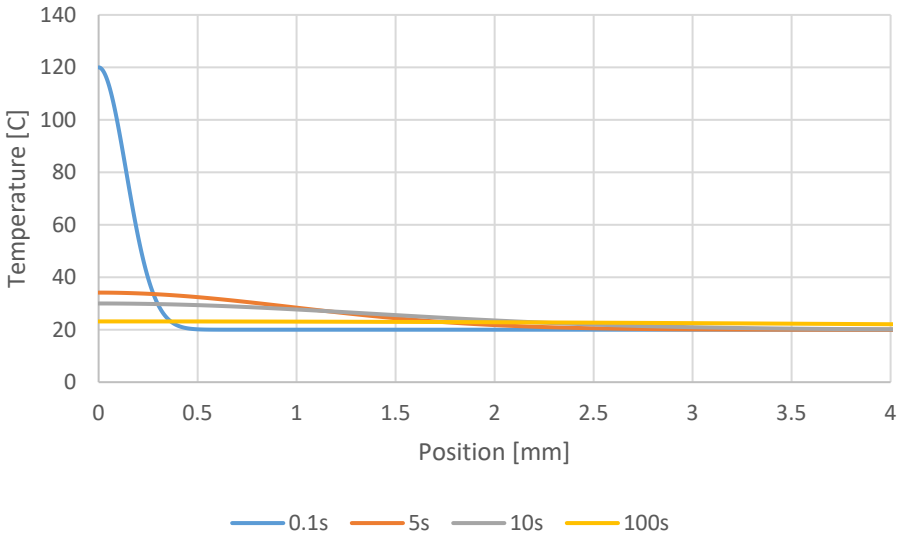

Figure 4. Prototype thermal analysis and simulation over time using single-layer parametric representation, Model 1, of a multilayer system. This graph is of the form of the classical heat-kernel solution where the medium extends from negative infinity to positive infinity.

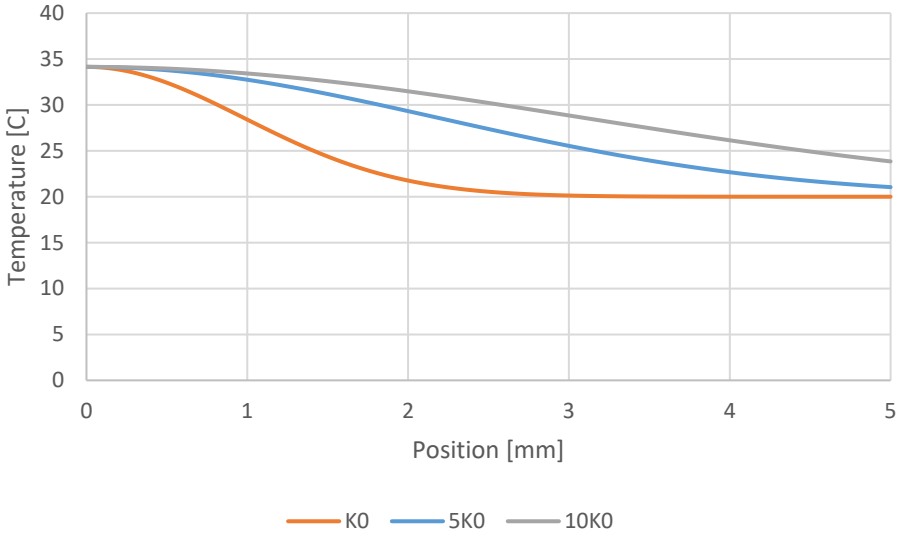

Figure 5. Prototype thermal analysis and simulation using single-layer parametric representation, Model 1, of a multilayer system at time equals 10s. This graph is of the form of the classical heat-kernel solution where the medium extends from negative infinity to positive infinity.

A more detailed estimate of the thermal response of a layered system, without the presence of a heat-sink layer, is by means of effective diffusivities averaged over two layers. This type of inverse analysis or simulation assumes prior knowledge concerning the relative values of effective diffusivities (i.e., that the diffusivity of one average layer is greater than that of the other). This type of thermal-response estimation is described in Figure 5, where the effective diffusivities κ_0 and κ_1, are assumed to be determined according to experimentally measured boundary values T_H and T_L, in the case of inverse analysis, or to be values within a parameter space, in the case of system simulation. In the case of Model 1, κ_0 and κ_1 are assumed to be similar enough such that effects of large changes in thermal diffusivity, Model 2, can be disregarded.

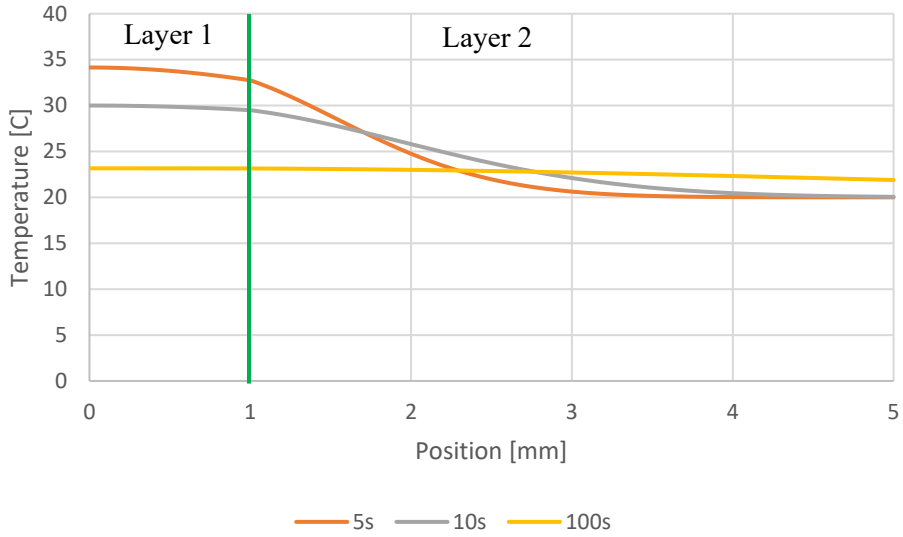

Figure 6. Prototype thermal analysis and simulation using double-layer parametric representation, Model 1, of a multilayer system where layer 1 (-∞ mm to 1 mm) is semi-infinite and layer 2 extends to infinity in the half-space. The thermal diffusivity of layers 1 and 2 are κ_1 $(10 \cdot \kappa_0)$ and κ_0, respectively.

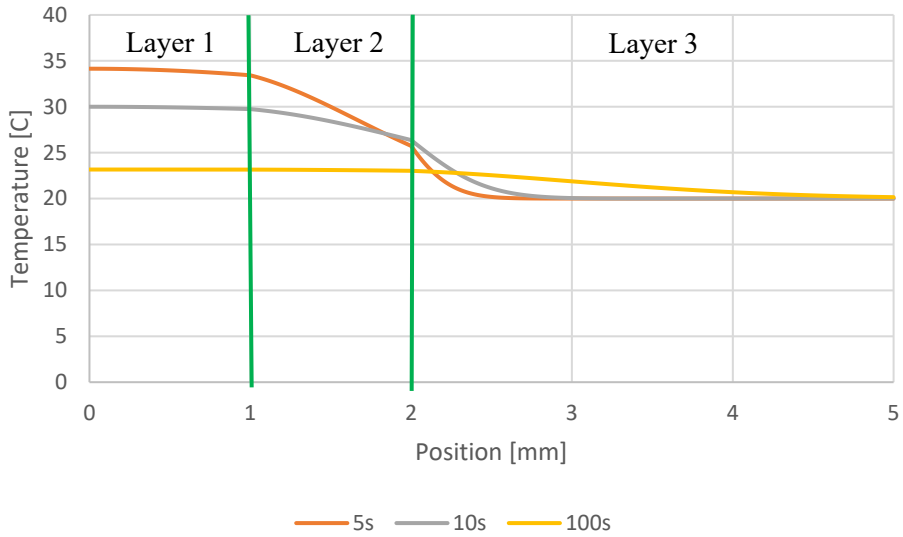

Figure 7. Prototype thermal analysis and simulation using triple-layer parametric representation, Model 1, of a multilayer system where layer 1 (-∞ mm to 1 mm) is semi-infinite, Layer 2 (1 mm to 2 mm) is finite, and layer 3 extends to infinity in the half-space. The thermal diffusivity of layers 1, 2, and 3 are $10 \cdot \kappa_0$, κ_0, and $0.1 \cdot \kappa_0$, respectively.

Next, an estimate of the thermal response of a layered system, where there exists a single heat-sink layer, is determination of an effective diffusivity averaged over the layered system and an effective diffusivity for coupling of the heat sink to the layered system. This type of thermal-response estimation is described in Figures 7-9, where the effective diffusivities κ_k and κ_s are assumed, with respect to inverse analysis, to be determined according to experimentally measured boundary values T_H and T_L and an initial estimate of the layered-material diffusivity. Consistently, Figures 7-9 can also describe a simulation where the effective diffusivities κ_k and κ_s are assumed to be values within a parameter space, which is a complex function of process variables.

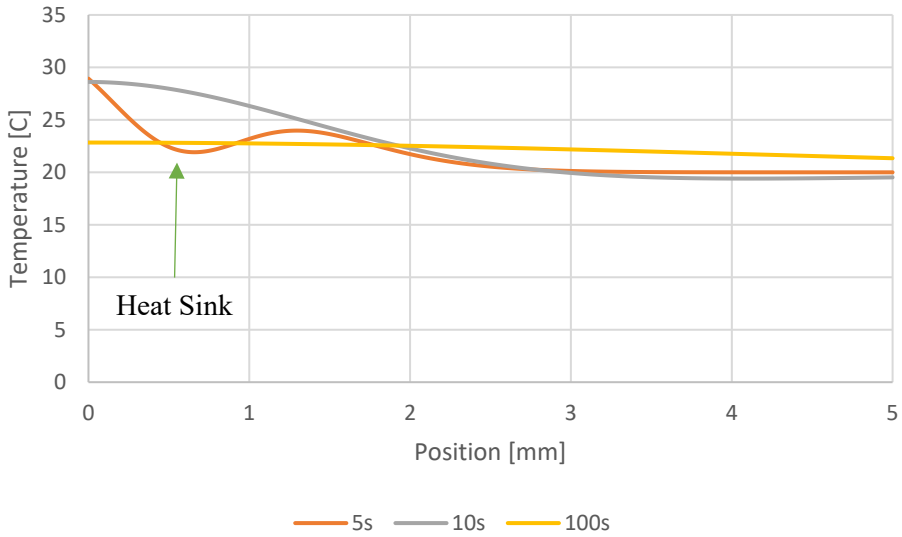

Figure 8. Prototype thermal analysis and simulation using single-layer parametric representation with the inclusion of a heat-sink, Model 1, of a multilayer system where the layer extends from negative infinity to positive infinity in the half-space. The thermal diffusivity of the heat sink is $10 \cdot \kappa_0$, and Cs corresponds to a ΔT of $10^{O}C$. The heat sink is located at 0.5mm, and turns on at t_s equals 4.9s.

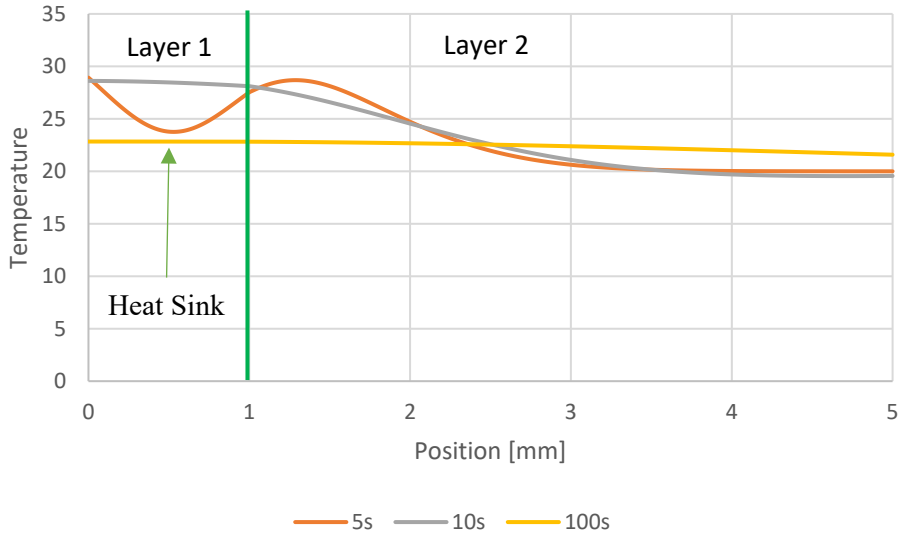

Figure 9. Prototype thermal analysis and simulation using double-layer parametric representation with the inclusion of a heat-sink, Model 1, of a multilayer system where layer 1 (-∞ mm to 1 mm) is semi-infinite and layer 2 extends to infinity in the half-space. The thermal diffusivity of layers 1 and 2 are $10 \cdot \kappa_0$ and κ_0, respectively. The thermal diffusivity of the heat sink is $10 \cdot \kappa_0$, and Cs corresponds to a ΔT of $10^{O}C$. The heat sink is located at 0.5 mm, and turns on at t_s equals 4.9s.

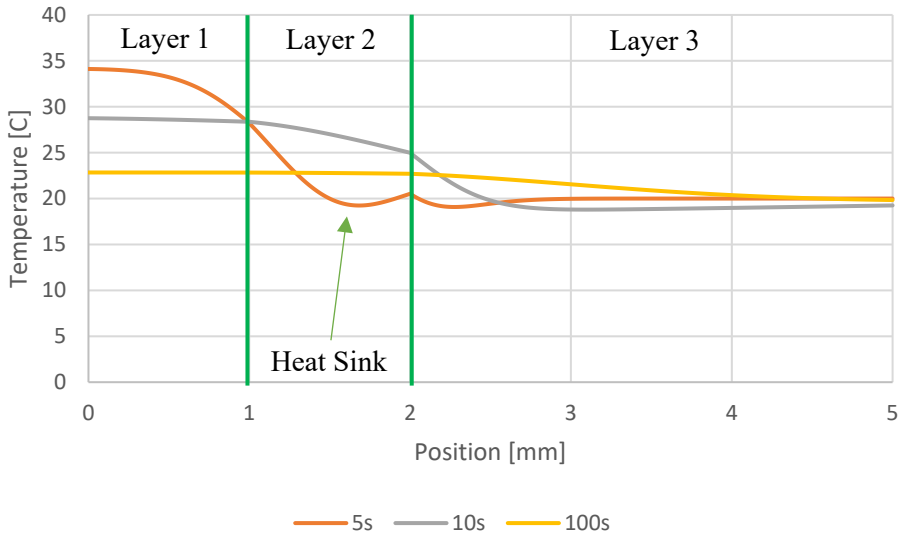

Figure 10. Prototype thermal analysis and simulation using triple-layer parametric representation with the inclusion of a heat-sink, Model 1, of a multilayer system where layer 1 (-∞ mm to 1 mm) is semi-infinity, Layer 2 (1 mm to 2 mm) is finite, and layer 3 extends to infinity in the half-space. The thermal diffusivity of layers 1, 2, and 3 are $10 \cdot \kappa_0$, κ_0, and $0.1 \cdot \kappa_0$, respectively. The thermal diffusivity of the heat sink is $10 \cdot \kappa_0$, and Cs corresponds to a ΔT of $10^{O}C$. The heat sink is located at 1.5 mm, and turns on at t_s equals 4.9s.

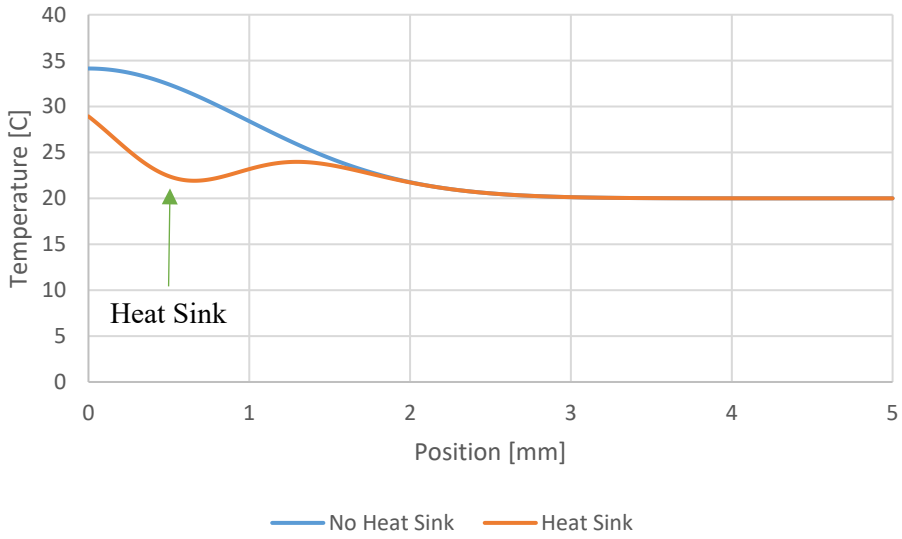

Figure 11. Prototype thermal analysis and simulation, at time equals 5s, using single-layer parametric representation, Model 1, of a multilayer of a multilayer system where the layer extends from negative infinity to positive infinity in the half-space. The thermal diffusivity of the heat sink is $10 \cdot \kappa_0$, and Cs corresponds to a ΔT of $10^{O}C$. The heat sink is located at 0.5 mm, and turns on at t_s equals 4.9s.

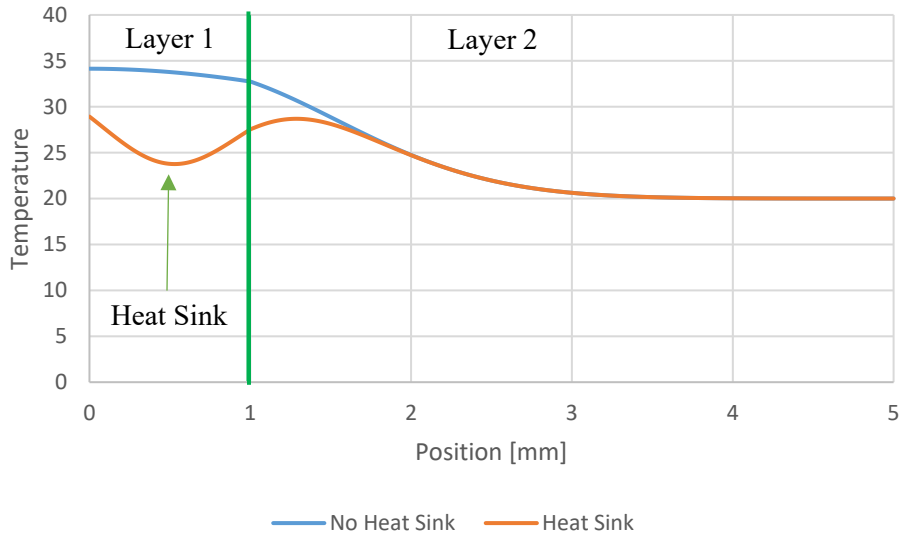

Figure 12. Prototype thermal analysis and simulation, at time equals 5s, using the double-layer parametric representation, Model 1, of a multilayer of a multilayer system where layer 1 (-∞ mm to 1 mm) is semi-infinite and layer 2 extends to infinity in the half-space. The thermal diffusivity of the heat sink is $10 \cdot \kappa_0$, and Cs corresponds to a ΔT of 10^{O}C. The heat sink is located at 0.5 mm and turns on at t_s equals 4.9s.

***Model* 2.** A more detailed estimate of the thermal response of a layered system, without the presence of a heat-sink layer, considers the effects of large changes in thermal properties between layers or the effects of contact resistance between layers. As stated previously, this type of inverse analysis or simulation assumes prior knowledge concerning the relative values of effective diffusivities (i.e., that the diffusivity of one average layer is greater than that of the other). This type of thermal-response estimation is described in Figures 13 and 14, where the effective diffusivities, κ_k, are assumed to be determined according to experimentally measured boundary values T_H and T_L, in the case of inverse analysis, or to be values within a parameter space, in the case of system simulation. . Note that in the following simulations, Figures 13-17, that the first layer extends to negative infinity, and the last layer extends to positive infinity. The graphs have been clipped at a specified distance for graphical presentation purposes.

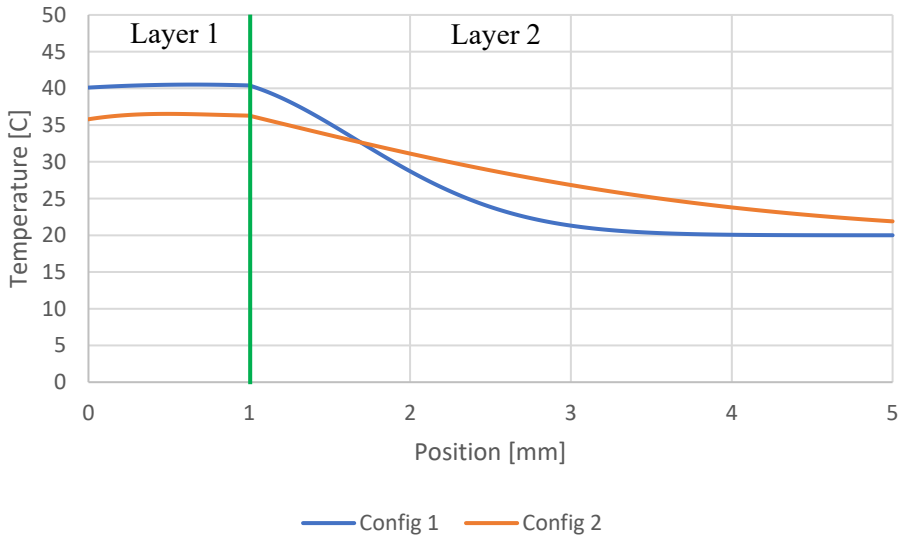

Figure 13. Prototype thermal analysis and simulation, at time equals 5s, using double-layer parametric representation, Model 2, of a multilayer system where layer 1 is semi-infinite (-∞ mm to 1 mm) and layer 2 extends to infinity in the half-space. The thermal diffusivity of layers 1 and 2 are $10 \cdot \kappa_0$ and κ_0 for configuration 1 and κ_0 and $10 \cdot \kappa_0$ for configuration 2, respectively.

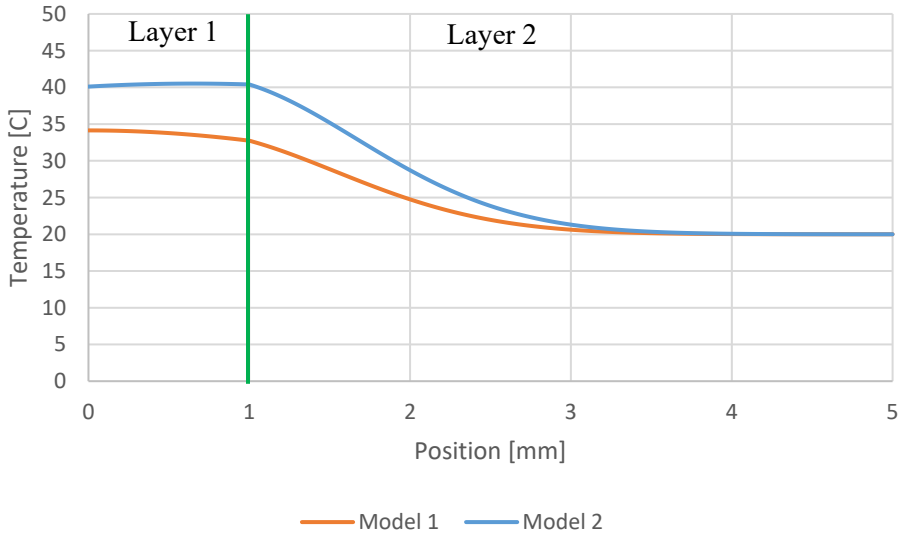

Figure 14. Prototype thermal analysis and simulation, at time equals 5s, using double-layer parametric representation, for both Model 1 and 2, of a multilayer system where layer 1 is semi-infinite (-∞ mm to 1 mm) and layer 2 extends to infinity in the half-space. The thermal diffusivity of layers 1 and 2 are $10 \cdot \kappa_0$ and κ_0, respectively.

Figure 15, 16, and 17 show the thermal response of the system, presented in Figures 11 and 12, with the inclusion of a heat-sink layer, where the effective diffusivities κ_k and κ_s, are assumed to be determined according to experimentally measured boundary values T_H and T_L, in the case of inverse analysis, or to be values within a parameter space, in the case of system simulation.

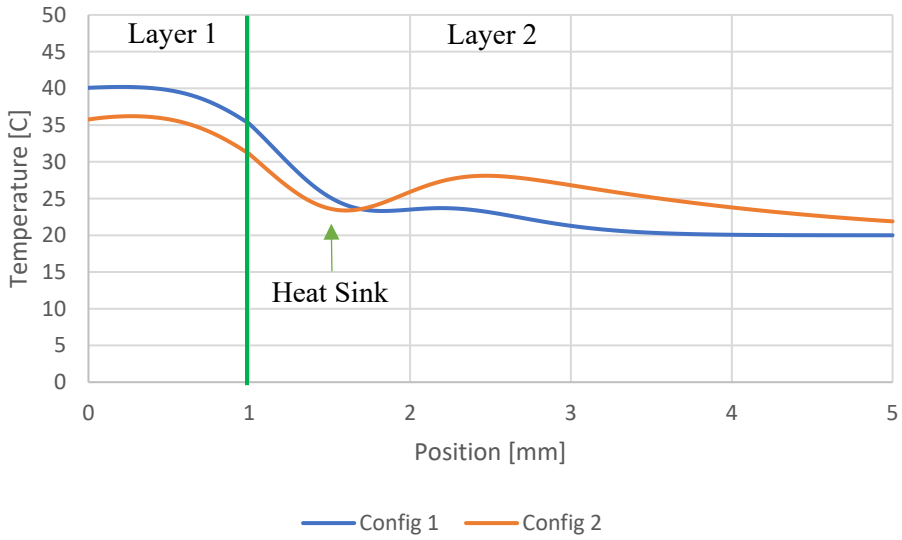

Figure 15. Prototype thermal analysis and simulation, at time equals 5s, using double-layer parametric representation with the inclusion of a heat-sink, Model 2, of a multilayer system where layer 1 is semi-infinite (-∞ mm to 1 mm) and layer 2 extends to infinity in the half-space. The thermal diffusivity of layers 1 and 2 are $10 \cdot \kappa_0$ and κ_0 for configuration 1 and κ_0 and $10 \cdot \kappa_0$ for configuration 2, respectively. The thermal diffusivity of the heat sink is $10 \cdot \kappa_0$, and Cs corresponds to a ΔT of $10^{O}C$. The heat sink is located at 0.5 mm and turns on at t_s equals 4.9s.

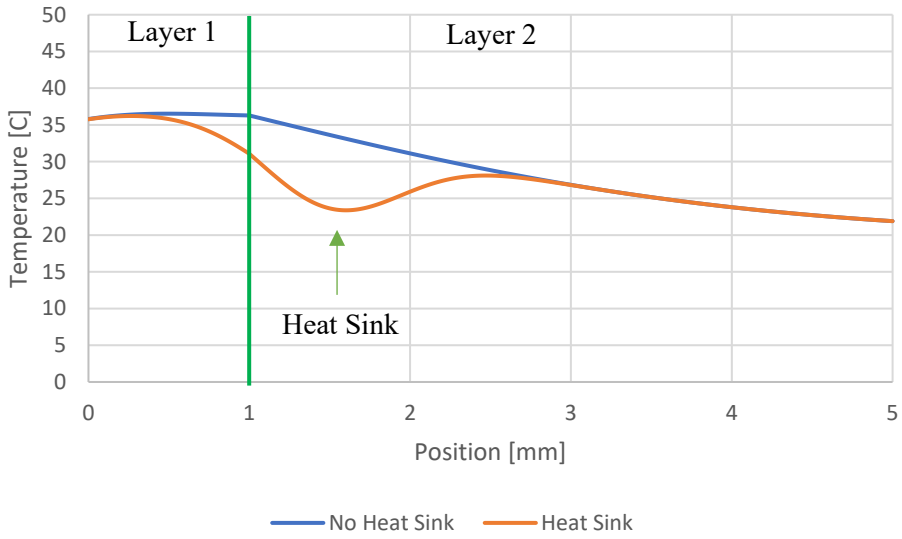

Figure 16. Prototype thermal analysis and simulation, at time equals 5s, using the double-layer parametric representation, Model 2, of a multilayer of a multilayer system where layer 1 (-∞ mm to 1 mm) is semi-infinite and layer 2 extends to infinity in the half-space. The thermal diffusivity of layers 1 and 2 are $10 \cdot \kappa_0$ and κ_0, respectively. The thermal diffusivity of the heat sink is $10 \cdot \kappa_0$, and Cs corresponds to a ΔT of $10^{O}C$. The heat sink is located at 1.5 mm and turns on at t_s equals 4.9s.

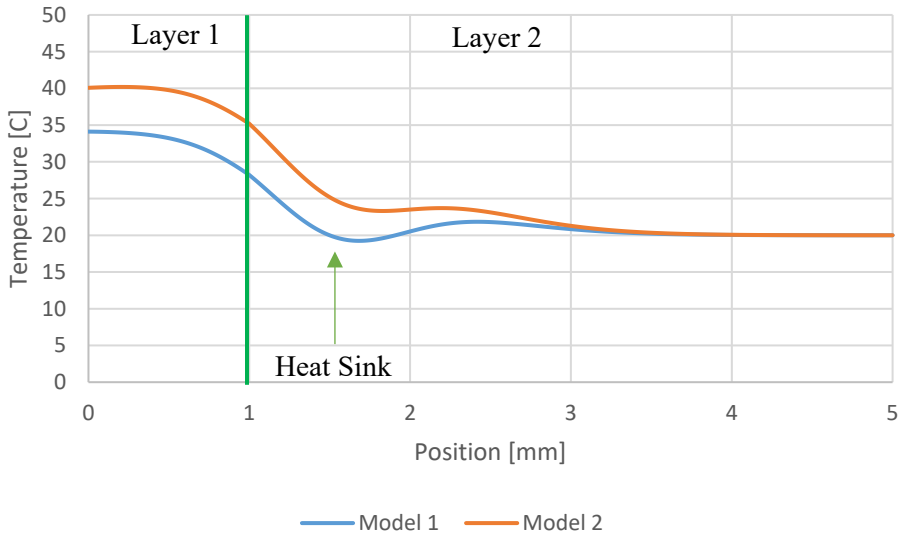

Figure 17. Prototype thermal analysis and simulation, at time equals 5s, using the double-layer parametric representation, for both Models 1 and 2, of a multilayer of a multilayer system where layer 1 (-∞ mm to 1 mm) is semi-infinite and layer 2 extends to infinity in the half-space. The thermal diffusivity of layers 1 and 2 are $10 \cdot \kappa_0$ and κ_0, respectively. The thermal diffusivity of the heat sink is $10 \cdot \kappa_0$, and Cs corresponds to a ΔT of $10^{O}C$. The heat sink is located at 1.5 mm and turns on at t_s equals 4.9s.

Discussion

For the prototype thermal analyses presented above, it was assumed that the heat source and heat sinks were thermal impulses represented by a delta function (i.e., the heat kernal solution), where the energy enters the domain and decays to the ambient temeprature as time approaches infinity. The results show that the addition of the heat sink term properly reduced the local temeprature fields and decayed to zero as time approached infinity. The additional layers added to the system demonstrated the effects of various materials and their interface effects on the temperature fields throughout the layered system.

Although not yet explicity included in these models other than as an effective diffusivity, another boundary value for thermal analysis and simulation is that of the heat-flux Q_L, which depends on material properties of the outer surface and ambient environment, Figure 16.

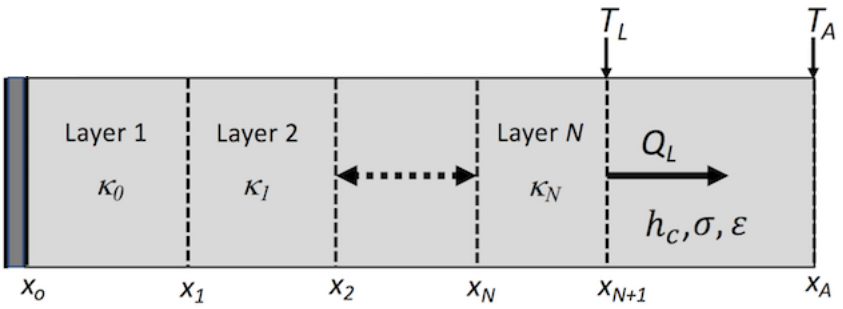

Figure 16. Schematic representation of heat-flux boundary condition Q_L on outer surface of layered-material system.

In particular, Q_L equals the rate of heat transfer between the outer surface and ambient environment due to convection (advection and diffusion) and thermal radiation, and may be expressed by

$$Q_L = h_c(T_L - T_A) + \varepsilon\sigma(T_L^4 - T_A^4) \qquad \text{Eq. 17}$$

Where h_c, ε, σ, and T_A are the convective heat-transfer coefficient, emissivity of the outer surface (e.g., 0.97 for polypropylene), Stefan-Boltzmann Constant ($5.6704 \cdot 10^{-8}$ $W \cdot m^{-2} \cdot K^{-4}$, and the ambient-environment temperature, respectively. The second term in Eq. 17 is the Stefan-Boltzmann-Law model of radiant heat [12]. For design optimization of layered material systems with respect to heat transfer, one seeks to minimize the difference T_L - T_A.

The prototype thermal analyses, using Models 1 and 2, adopt effective diffusivities and equivalent sources. This separation of parameters may provide some insight concerning the scaling of effective diffusivities relative to estimated bulk heat-transfer properties of materials comprising a layered system. Formally, however, the quantities $C(x_0)/\sqrt{4\pi\langle\kappa_0\rangle}$ and $C_s(x_s)/\sqrt{4\pi\langle\kappa_s\rangle}$ are not independent parameters, and for inverse thermal analysis and simulation, they may be combined phenomenologically into single adjustable parameters $C(x_0)$ and $C_s(x_s)$, respectively.

Formally, Models 1 and 2 also provide parametric representation of heat transfer through layered material system where effective diffusivities are functions of position within layers. This follows in that Eqs. 5 and 12 of Models 1 and 2, respectively, can be adopted for approximate discrete representation of effective diffusivities whose forms are that of continuous functions.

General features of the parametric Models 1 and 2 were presented in this study with respect to thermal analysis and simulation. As previously described, given that a parameter space has been generated for a given system, a selected parametric model can be used for system simulation and prediction of required parameters to achieve a given target temperature field. For example, the calculations shown in Figures 13 and 14 can be interpreted as prototype simulations of heat sink properties required to achieve a target temperature at a position, x_s, in space, given that a parameter space of encoded thermal response properties is available. In principle, this parameter space would include effective diffusivities for different layered and heat sink materials, for a sufficient range of boundary conditions.

As discussed in the introduction, heat transfer within the heat-sink layer, along scale l_1 described schematically in Figure 1, is that of a thin-layer material, interface-coupled to adjacent material surfaces. In general, experimental measurement and modeling of temperatures within this layer are for a temperature field spanning a two-dimensional surface, which is coupled to a cooling bath at specified locations along its edge. Development of parametric-model representations of this temperature field, which is on a different scale than that of heat transfer through a multilayer system, poses a separate problem, and is dependent on the system of interest.

Conclusion

Determination of optimal process parameters for achieving a given target temperature field for heat transfer through a layered material using layer configurations and heat sinks poses a specific problem. The results of this study demonstrate use and general features of parametric models, whose parameterization should provide convenient generation of parameter spaces for optimization of layered materials with respect to target heat-transfer characteristics. These models consist of general parametric representations that are structured for further extension and modification, which should be the focus of future studies. Further studies should also investigate hot boundary sources where the energy introduced to the system is not that of a single delta function impulse.

Acknowledgement

This work is supported by U.S. Special Operations Command, Special Operations Forces Acquisition, Technology, and Logistics (USSOCOM SOF AT&L).

References

1. S.G. Lambrakos, “Parametric Modeling of Welding Processes Using Numerical-Analytical Basis Functions and Equivalent Source Distributions,” Journal of Materials Engineering and Performance, Volume 25(4), April 2016, pp. 1360-1375.
2. E. Michaelchuck Jr., S. Ramsey, T. Mayo, S.G. Lambrakos. “Experimental Proof of Concept for Heat Sink-Controlled Temperature Fields within Multi-Layered Materials,” NRL Memorandum report (in progress).
3. H. S. Carslaw and J. C. Jaegar: Conduction of Heat in Solids, Clarendon Press, Oxford, 2nd ed, 374, 1959.
4. A. Tarantola, “Inverse Problem Theory and Methods for Model Parameter Estimation,” SIAM, Philadelphia, PA, 2005.
5. M.N. Ozisik and H.R.B. Orlande: Inverse Heat Transfer, Fundamentals and Applications, Taylor and Francis, New York, 2000.
6. K. Kurpisz and A.J. Nowak: Inverse Thermal Problems, Computational Mechanics Publications, Boston, USA, 1995.
7. O.M. Alifanov, Inverse Heat Transfer Problems, Springer, Berlin, 1994.
8. J.V. Beck, B. Blackwell, C.R. St. Clair, Inverse Heat Conduction: Ill-Posed Problems, Wiley Interscience, New York, 1985.
9. J.V. Beck, “Inverse Problems in Heat Transfer with Application to Solidification and Welding,” Modeling of Casting, Welding and Advanced Solidification Processes V, M.

Rappaz, M.R. Ozgu and K.W. Mahin eds., The Minerals, Metals and Materials Society, 1991, pp. 427-437.
10. J.V. Beck, “Inverse Problems in Heat Transfer,” Mathematics of Heat Transfer, G.E. Tupholme and A.S. Wood eds., Clarendon Press, (1998), pp. 13-24.
11. S.V. Patankar, Numerical Heat Transfer and Fluid Flow, Series in Computational Methods in Mechanics and Thermal Sciences, Hemisphere Publishing Corporation, London, 1980.
12. C.F. Bohren, F. Craig and D.R. Huffman, Absorption and Scattering of Light by Small Particles, Wiley (1998), pp. 123–126.